ELSEVIER

Biophysical Chemistry 125 (2007) 320–327

Biophysical Chemistry

http://www.elsevier.com/locate/biophyschem

Solution behavior of a sugar-based carborane for boron neutron capture therapy: A nuclear magnetic resonance investigation

Claudia Bonechi [a], Sandra Ristori [b], Silvia Martini [a], Luigi Panza [c], Giacomo Martini [b], Claudio Rossi [a], Alessandro Donati [a,*]

[a] *Dipartimento di Scienze e Tecnologie Chimiche e dei Biosistemi, Università di Siena, via A. Moro 2, 53100 Siena, Italy*
[b] *Dipartimento di Chimica, Università di Firenze, via della Lastruccia 3, 50019 Sesto Fiorentino, Firenze, Italy*
[c] *Dipartimento di Scienze Chimiche, Alimentari, Farmaceutiche, Farmacologiche , Università degli Studi del Piemonte Orientale, viale Ferrucci 33, 28100 Novara, Italy*

Received 18 July 2006; received in revised form 10 September 2006; accepted 10 September 2006
Available online 31 October 2006

Abstract

The physico-chemical properties of *β*-lactosyl-*closo*-*ortho*carborane in water solution were investigated by multinuclear NMR, ^{13}C NMR relaxation, and *ab-initio* calculations. This molecule represents a potentially selective boron carrier in Boron Neutron Cancer Therapy (BNCT) and exhibits amphiphilic characteristics. Its structural and dynamic features were studied comparing NMR data acquired in both aggregating and non-aggregating conditions. Aggregates are characterized by rapid exchange with the bulk and by high sensitivity to temperature conditions. An unusually stable intra-molecular CH···O hydrogen bond was found to persist in water solution both for the free molecules and after aggregate formation. At the same time, inter-molecular specific CH···O interactions do not seem effective in the aggregate formation process, which appears to take place only on non-specific hydrophobic basis.

Keywords: Carborane; BNCT; ^{13}C relaxation rate; Carborane aggregates; C–H···O hydrogen bond

1. Introduction

Polyhedral boranes and heteroboranes have been the subject of widespread interest for at least 50 years and this was mainly due to the ability of boron atoms to catenate and form molecular networks with rather peculiar geometries [1]. In several cases aromatic-like electronic features were observed [2]. Recently, dicarba-*closo*-dodecaboranes ($C_2B_{10}H_{12}$) and their derivatives have found application in biological and medical fields [3–5]. Among the medical applications, of particular interest is Boron Neutron Capture Therapy (BNCT) [6–8], a targeted cancer treatment based on borocompound administration to patients and subsequent exposure to an epithermal neutron beam. Indeed ^{10}B nuclei, due to their large neutron absorption cross section, are able to undergo fission:

$$^{10}B + {}^{1}n \rightarrow {}^{7}Li + {}^{4}He$$

This generates heavy particles with a few μm penetration length in tissues, which allows the ionising products of the reaction, i.e. mainly ^4He particles, to damage almost exclusively the cells where they are located, or those in the nearest proximity. Potential BNCT agents have to fulfil several requirements, depending on the type of tumour to be treated, the administration procedure, and the possible use of carriers. The most important feature is the preferential localization of borocompounds in malignant cells rather than in healthy tissues. In order to reach this goal, boron-containing molecules with some natural affinity for tumours, such as *p*-borophenylalanine (BPA) [9,10] and glycosyl-carboranes (GCs) [11,12], have been synthesized. BPA has been used in clinical trials, whereas GCs are promising candidates for BNCT [13,14].

* Corresponding author. Tel.: +39 0577 234370; fax: 39 0577 234177.
E-mail address: alessandro.donati@unisi.it (A. Donati).

0301-4622/$ - see front matter © 2006 Elsevier B.V. All rights reserved.
doi:10.1016/j.bpc.2006.09.004

In this paper we report a NMR study and a theoretical density functional calculation of the [1,2-dicarba-*closo*-dodecaboran (12)-1-yl-methyl](*β*-D-galacto-pyranosyl)-(1→4)-*β*-D-glucopyranoside molecule (LCOB, Fig. 1).

LCOB is a carboranyl carbohydrate composed of a lipophilic boron icosahedral cage and a hydrophilic lactosyl moiety. The intrinsic amphiphilic nature of glycosyl-carboranes let us expect aggregate formation in aqueous media, which has, in fact, been observed at concentration higher than $6 \div 7 \times 10^{-4}$ mol/dm^3, the exact value depending on the ionic strength and temperature [15]. This meant that we could easily insert these molecules in liposome [15–17] and/or conceive the direct use of self-produced micelles as boron vectors.

Nuclear Magnetic Resonance has proven to be a suitable technique for the physico-chemical characterization at a molecular or micellar level, and it has been used since long to obtain valuable information on surfactant-based systems [18–20]. The analysis of the structural and dynamical properties of LCOB, obtained by this approach in both aggregating and non-aggregating conditions, can be of interest to understand the inter-molecular interactions that are responsible for LCOB supra-molecular organization in water.

2. Experimental

2.1. Samples

High grade pure water was obtained from a Milly-Q (Millipore) apparatus. Deuterated water (99.95% purity) was purchased from ISOTECH (Matheson USA Co., Ohio, USA). C_2D_5OD (99.95% isotopical composition) and $CDCl_3$ (99.95% purity) were purchased from Carlo Erba (Milan, Italy) and from Merck, Darmstadt, Germany, respectively. [1,2-dicarba-*closo*-dodecaboran(12)-1-yl-methyl](*β*-D-galactopyranosyl)-(1→4)-*β*-D-glucopyranoside (Fig. 1, LCOB or lactosyl-carborane) was prepared as described elsewhere.[12]

2.2. Nuclear magnetic resonance methods

NMR experiments were performed on a Bruker DRX-600 AVANCE spectrometer equipped with an *xyz* gradient unit, operating at 600.13 MHz, 150.89 MHz and 192.50 MHz for ^{1}H, ^{13}C and ^{11}B, respectively. Most of the experiments were acquire with a Bruker TBI reverse triple resonance (^{1}H, ^{13}C, Broad Band) probe with *xyz* gradients. ^{11}B spectra and ^{13}C inversion recovery experiments were acquired with a Bruker BBO double resonance (^{1}H, Broad Band) probe with *z* gradients.

Experiments acquired at low LCOB concentration were performed on a Bruker AVANCE 500 spectrometer, operating at 500.23 MHz for ^{1}H and 125.79 MHz for ^{13}C and equipped with a dual ^{13}C {^{1}H} CryoProbe.

^{1}H–{^{11}B} NOESY [21], ROESY [22], and ^{1}H{^{11}B}–^{1}H {^{11}B} dqf-COSY [23] spectra were acquired with 2048 complex points for 256 experiments with 8 s recycle time and TPPI [24] phase cycling. ^{11}B broad band decoupling was applied by using a GARP [25] composite-pulse sequence. Zero filling and other common data processing were applied. NOESY spectra were acquired with mixing times of 100, 200, 400 ms. ROESY spectra were acquired with mixing times of 200 ms. Sensitivity enhanced ^{1}H–^{13}C HSQC spectra [26] were acquired with 2048 complex points for 256 experiments and hyper-complex phase cycling [27].

^{13}C spin-lattice relaxation time (T_{1C}) was measured using an "inversion recovery" [28] with gate decoupling pulse sequence. Data analysis was performed using a three parameter exponential regression to fit the longitudinal magnetization recovery curve. The variable delay was: 0.005, 0.01, 0.02, 0.04, 0.08, 0.1, 0.2, 0.4, 0.8, 1.0, 1.5, 2.5, 5.0, 8.0, 15.0 s with a recycle time (d_1) of 15 s. The experimental error for the longitudinal relaxation rate R_1 was within 5%. ^{11}B spectra were referenced to a freshly prepared KBF_4/D_2O solution. ^{1}H decoupling was obtained by using a WALTZ-16 composite-pulse sequence [29].

Data were processed with Bruker XWinNmr software and NMRpipe [30] software (3.3 version). 2D spectra were analyzed by using SPARKY package [31]. Integration of the cross-peak volumes in NOESY spectrum was done using the Gaussian-fitting algorithm of SPARKY.

2.3. Theoretical calculation

Density functional calculations (DFT) were performed on the isolated molecule by Gaussian03 package [32] implemented

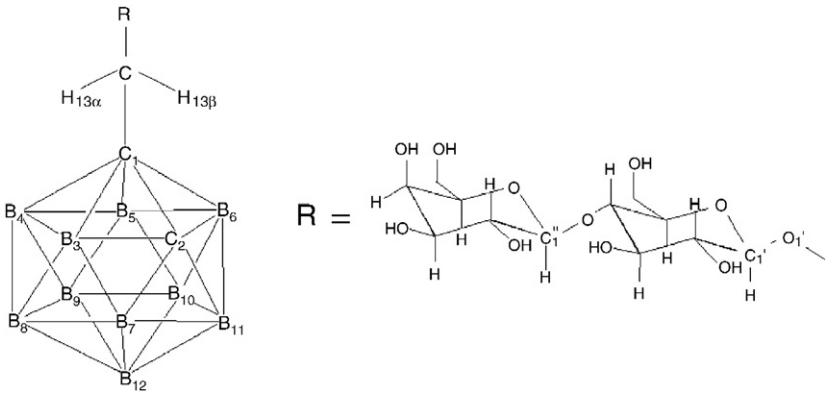

Fig. 1. Structure of [1,2-dicarba-*closo*-dodecaboran(12)-1-yl-methyl](*β*-D-galactopyranosyl)-(1→4)-*β*-D-glucopyranoside (LCOB). For the sake of clarity hydrogen atoms have been omitted in the carborane cage. Numbering is shown only for first carbons of glucose and galactose of the disaccharide.

on a IBM SP5/512 supercomputer [33]. Geometry optimisations were obtained by B3LYP method at 6–31G** level.

3. Results and discussion

3.1. ^{1}H, ^{13}C and ^{11}B assignments

The complete assignment of the ^{1}H NMR spectrum of LCOB in D_2O in both aggregating [LCOB > $6–7\times10^{-4}$ mol/dm^3] [15] and non-aggregating conditions [LCOB < $6–7\times10^{-4}$ mol/dm^3] was done by using a set of NMR experiments: $^{1}H–\{^{11}B\}$ NOESY, $^{1}H\{^{11}B\}–^{1}H\{^{11}B\}$ dqf-COSY, $^{1}H–^{13}C$ HMQC, and $^{11}B\{^{1}H\}$ (details of assignment are reported in Supporting information).

Fig. 2 reports the NMR proton spectra of LCOB at two different concentrations in D_2O. The spectrum at [LCOB] = 2.0×10^{-4} mol/dm^3 (Fig. 2A) was recorded with a cryo-probe in order to obtain a better signal-to-noise ratio. In this case ^{11}B decoupling was not possible, because the experimental set-up did not allow simultaneous irradiation at the boron frequency. The region of protons bound to boron atoms (H–B) between 2.0 ppm and 2.4 ppm, is shown in the enlargement. This portion of the spectrum contained four broad peaks of relative intensity 2:2:1:5 assigned to $H_{3/6}$ (2.348 ppm), $H_{4/5}$ (2.148 ppm), H_9 (2.136 ppm), $H_{8/10}$, H_{12} (2.100 ppm) and $H_{7/11}$(2.075) of the carborane cage, respectively. The diastereotopic protons of the bridge were easily recognised on the basis of their mutual strong COSY and NOESY cross-peaks observed at 4.16/4.32 ppm (Supporting information and Fig. 3B, respectively). No dipolar connection between the $H_{13}(\alpha,\beta)$ bridge protons and H_2 (Fig. 3A) was observed, indicating that they are not in close contact. $H_{13}(\alpha,\beta)$ were only coupled to the proton pair $H_{4/5}$ resonating at 2.149 ppm. This behaviour was similar to what we found in C_2D_5OH as solvent [34], where the formation of persistent CH···O bond in solution hinder the free rotation around the $C_1–C_{13}$ bond. The remaining ^{1}H together with the ^{13}C resonances were assigned on the basis of the dqf-COSY and $^{1}H–^{13}C$ HMQC spectra.

The ^{11}B NMR spectrum of lactosyl-carborane in water solution consisted of 5 peaks at −4.29, −6.08, −10.46, −12.72 and −14.05 ppm, with intensity ratio 1:1:4:2:2 (Supporting information). They were attributed, on the basis of previous literature [35], to B_9, B_{12}, $B_{4/5/8/10}$, $B_{3/6}$ and $B_{7/11}$, respectively. No appreciable changes (both for chemical shift and line-width) were observed at different concentrations in the range between 1.0×10^{-3} mol/dm^3 and 2.0×10^{-2} mol/dm^3 in D_2O.

3.2. Structural and dynamic analysis

The structural and dynamic studies of LCOB in water solution presented some remarkable aspects, connected with aggregate formation and with the occurrence and persistence of the CH···O hydrogen bond [36]. The comparison between the free and aggregate forms could give information about the intermolecular interaction with special focus on the role played by the carborane CH. The ability of this polarized CH to drive the

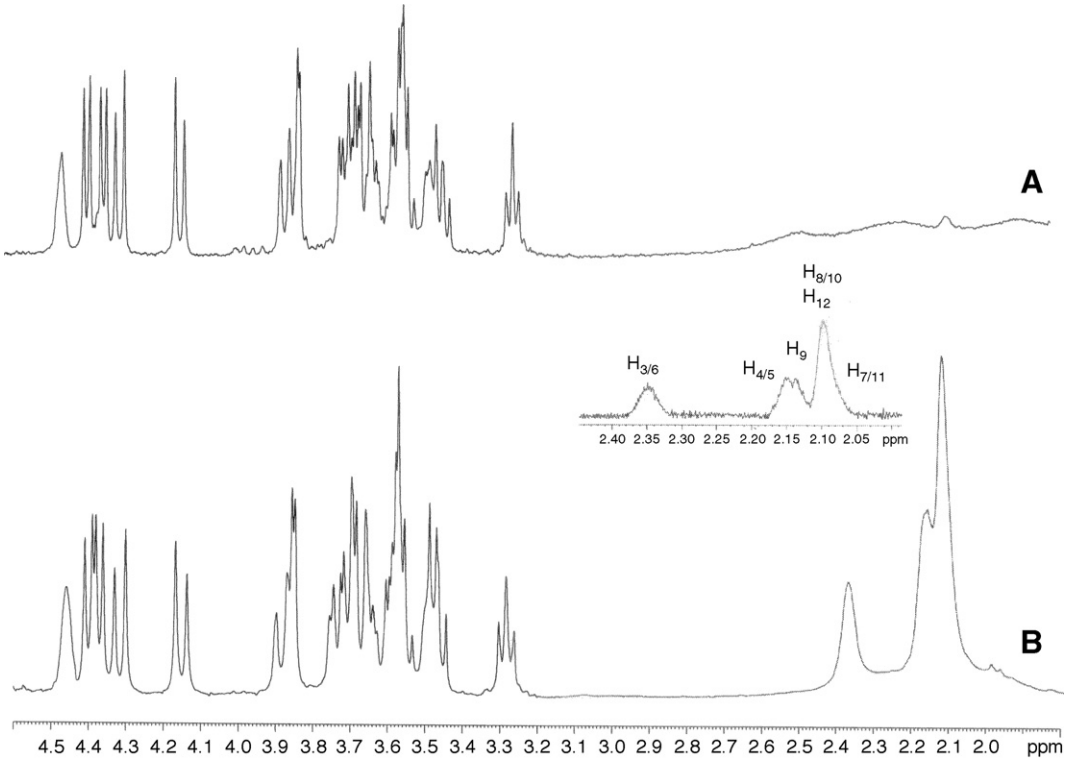

Fig. 2. (A) Proton NMR spectrum of [LCOB] = 2×10^{-4} mol/dm^3 in D_2O recorded with a cryo-probe at 500 MHz, no ^{11}B decoupling and 298 K. (B) $^{1}H\{^{11}B\}$ NMR spectrum of [LCOB] = 2×10^{-2} mol/dm^3 in D_2O recorded at 600 MHz and 298 K. In the insert, the region between 2.4 ppm and 2.0 ppm of spectrum (B) is shown. In this case the different signal-to-noise ratio is due to a sine-bell squared multiplication function, used to increase resolution.

formation of supra-molecular complexes was already recognised in the solid state [37]. At the same time, the possible rearrangement of intra- and inter-molecular hydrogen bonds network, should confer different dynamic properties to the different segments of the molecule, which was interesting especially with regard to the aggregate formation mechanisms. Additional information could be extracted in relation to the uncommon strength of bond. Here its persistence upon aggregate formation confirmed that CH···O bond energy is comparable with that of classic hydrogen bonds.

In order to develop these points and to establish geometrical constrains for the structure of the molecule, a set of mono- and bi-dimensional NMR spectra and ^{13}C non-selective relaxation experiments were performed and analysed in both aggregating and non-aggregating conditions. Previous quasi-elastic light scattering (QELS) and electron spin resonance (ESR) experiments suggested that at 2.0×10^{-4} mol/dm^3 no aggregation occurs [15]. The $^1H-\{^{11}B\}$ NMR spectrum in D_2O, at the same concentration, was in line with this finding (Fig. 2A). In fact, the typical narrow line NMR spectrum was recorded and was attributed to the free monomer species in solution. A similar line-width for all ^1H peaks, (H–C and H–B), was observed in the spectra taken in C_2D_5OD and $CDCl_3$.

The $^1H-\{^{11}B\}$ NMR spectrum recorded at high concentration (2.0×10^{-2} mol/dm^3) in D_2O, at which aggregate formation was clearly established [15], did not present significant differences for both chemical shifts and line-widths (Fig. 2B). We also did not detect meaningful variation in the ^{11}B spectrum when passing from aggregating to non-aggregating conditions (in this case non-aggregating conditions were achieved in C_2D_5OD; Supporting information).

This result was quite unexpected. In fact, nuclear transverse relaxation (especially for quadrupolar nuclei) is known to be very sensitive to different motional conditions [38]. Therefore, the line-shape of ^1H–B and ^{11}B should present relatively large variation upon aggregate formation. Chemical shift should also be sensitive to aggregation.

On the other hand, large and roughly spherical objects with an average size 10–15 nm were detected by cryo-TEM micrographs taken in similar conditions (2.0×10^{-2} mol/dm^3 in buffered water) [16]. The size of these aggregates was inconsistent with the rapid motion deducible from the sharp NMR peaks [38]. We thus considered a dynamic model in which monomers underwent to rapid exchange with the aggregates. In this case, the NMR spectra were the weighted average between the signals of the rapid tumbling bulk molecules and the signals of free molecules, whose motion was modulated (slowed) by the exchange with the aggregates. Signals of molecules inserted in the aggregates were strongly broaden, resulting NMR—undetectable. The fact that only free molecules were observed, also could be interpreted as a reduction of the motion of monomers inside aggregates. This could be due to the net of hydrogen bonds formed by hydroxyl groups of disaccharide lateral chains. In fact, a meaningful degree of "lateral diffusion" should lower transverse nuclear relaxation, giving broad but observable peaks in the NMR spectrum. These hypotheses were confirmed by NOESY and ^{13}C relaxation experiments which will be discussed hereafter.

The NOESY spectra of LCOB in D_2O in aggregating and non-aggregating conditions are reported in Figs. 3(A, B) and 4, respectively. From the comparison of the two spectra it was possible to observe that the relative sign of the cross-peaks dramatically changed passing from high to low LCOB concentration. In the presence of aggregates, well resolved cross-peaks with the same sign as the diagonal were obtained, whereas in non-aggregating conditions cross-peaks and auto-peaks showed opposite sign. The behaviour of the NOEs in the two states reflected two different motional conditions of LCOB in solution. In fact, when the extreme narrowing limit holds ($\omega\tau_c<1.12$) [39], NMR theory predicts that NOESY diagonal

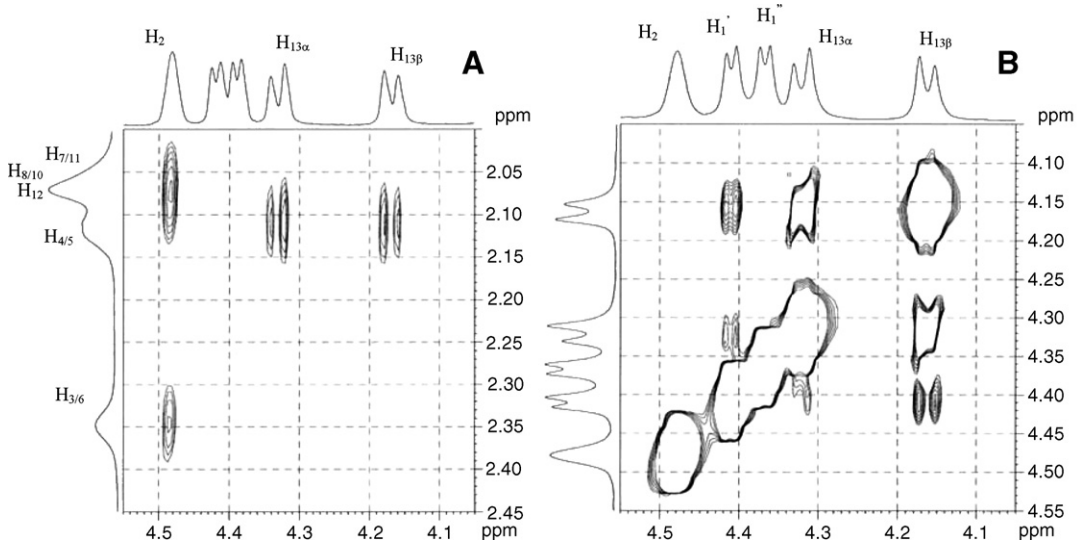

Fig. 3. NOESY spectrum of [LCOB]=2×10^{-2} mol/dm^3 in D_2O, acquired at 600 MHz with a mixing time of 200 ms and temperature of 298 K: (A) region of the H*B*-cage to the H_2C-bridge and to $H_{13(\alpha,\beta)}$ cross-peaks; (B) region of the H_2, anomeric and $H_{13(\alpha,\beta)}$ cross-peaks.

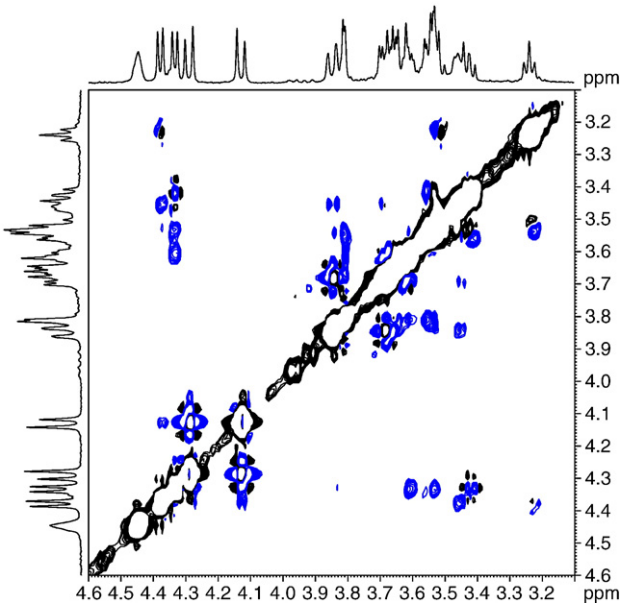

Fig. 4. NOESY spectrum of [LCOB]=2×10^{-4} mol/dm^3 in D_2O acquired at 298 K on a 500 MHz NMR instrument equipped with a cryo-probe (mixing time=200 ms). Blue cross-peaks are negative, diagonal peaks (black) are positive. (For interpretation of the references to colour in this figure legend, the reader is referred to the web version of this article.)

peaks have opposite sign with respect to cross peaks. On the contrary, when the molecules are in the slow motion regime ($\omega\tau_c > 1.12$) the sign of cross-peaks and auto-peaks are expected to be the same [40].

The comparison of NOESY spectra (Fig. C: supplementary material) of the same LCOB sample at high concentration, acquired at different temperatures (288 K and 308 K), also showed an inversion of the cross-peaks sign with respect to the diagonal peaks. This behaviour was remarkable, if considering that in a relatively small range of temperature (20 K) the motional regime underwent to such dramatic change. The above evidences confirmed the dynamic nature of the aggregates and indicated that LCOB aggregates easily exchanged their constituents with the bulk solution.

We also compared the ^{13}C relaxation behaviour of the two systems at various temperatures. For these experiments the non-aggregating state was studied in ethanol at high concentration (2.0×10^{-2} mol/dm^3) [41–45], in order to circumvent the sensitivity problem due to low natural isotopic abundance. However, this approximation on the physico-chemical conditions does not prevent the possibility to compare the relaxation behaviour of the two states.

The effect of the temperature on ^{13}C relaxation rates (R_{1C}) was very interesting. In water solution, at 2.0×10^{-2} mol/dm^3, that is in the presence of aggregates, a dual behaviour was observed for all carbon atoms in the molecule. In fact, R_{1C} increased from 283 K up to 298 K and then decreased at temperatures higher than 298 K (Fig. 5A). On the contrary, in ethanol solution, i.e. in the absence of aggregates, a monotonic decrease of R_{1C} with increasing temperature was observed (Fig. 5B). These experimental evidences suggested that the trend of the relaxation rates in water was due to the sum of different contributions: the increase of the isotropic tumbling for both isolated molecules and aggregates, and the kinetic enhancement of the exchange between the two states. In fact, at low temperature, the system consisted of free molecules in rapid exchange with slow tumbling aggregates. These aggregates modulated the relaxation time even if they were not directly detected by NMR. Rising the temperature caused both a more rapid motion in isolated molecules and the increase of the exchange rate between free molecules and aggregates, contributing to the enhancement of R_{1C} until its maximum at 298 K was reached. After this point, relaxation of isolated molecules dominated the resulting R_{1C} values, inducing a constant decrease of R_{1C}. On the other hand, the monotonic decrease of R_{1C} in C_2D_5OD solution meant that the system was in fast motional regime even at temperatures as low as 283 K. In this case, R_{1C} decreased with the decrease of the correlation time induced by higher temperatures. These results confirmed the hypothesis suggested above on the basis of NOESY data.

Noteworthy, differences in the relaxation behaviour were also observed in different parts of the molecule (Fig. 5): i) quaternary C_1 resulted almost unaffected by temperature changes, even if the observed trend was similar to the rest of the molecule; ii) the

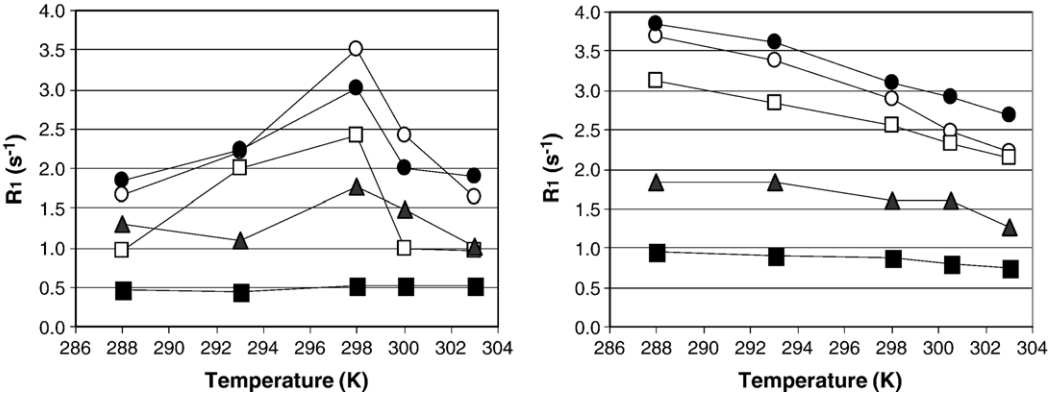

Fig. 5. ^{13}C relaxation rate (R_1) values versus temperature for LCOB in aggregating (*left*) and non-aggregating (*right*) conditions (see text for further details). For both the conditions, arithmetic mean values for all the carbons of galactose (●) and glucose (○) residues of lactose are presented. Values for the bridging C_{13} (▲) and the cage C_1(■) and C_2(□) are also reported.

average of R_1 values for galactose and glucose moieties were very similar, showing that segmental motion in the hydrophilic part of the molecule did not appreciably contribute to the relaxation mechanism; iii) carborane C_2 showed relaxation rates similar, even if slightly lower, to the sugar carbons (the average decrease was 35% and 10% for aggregating and non-aggregation condition respectively), suggesting that an isotropic correlation time dominated the relaxation. This moderate reduction of R_{1C} values observed for C_2 could be due to the increase of the C–H distance as a consequence of CH···O bond formation; iv) the low relaxation rates measured for the bridging C_{13} were not completely understandable. Indeed a fast libration could not be compatible with the CH···O bond formation.

Concerning the structural features of LCOB, to correctly consider conformational changes between free monomers and aggregates, we might take into account that NMR gave us a picture of the sole free molecules exchanging with aggregates. Thus we only got indirect information about what happened within aggregates themselves.

This condition can be expressed in terms of a simplified system in which two spins of the molecule (ligand) undergo two-site exchange between free and bound states, where both the kinetic exchange constants (forward k_1, and backward k_{-1}) are much higher than the ligand relaxation rate in the free (R_1^f) and bound state (R_1^b). Here transferred NOE could occur [46], giving information about the conformation of the ligand in the bound state by observing the ligand in the free state. However, no difference was observed in the NOE cross-peaks network between aggregating and non-aggregating conditions, confirming that the molecule did not appreciably change its conformation in the two states.

As briefly reported in the previous section, the comparison of the NOESY spectra obtained at different concentrations (Figs. 3 and 4) showed that the arrangement of the different molecular segments was preserved in passing from the monomer to the aggregate form. In fact, the absence of a cross-peak between H_2 and the diastereotopic methylenic protons $H_{13\alpha,\beta}$, as well as the presence of NOE interactions between $H_{13\alpha,\beta}$ and the $H_{4/5}$ protons, confirmed that the orientation of the carborane cage was fixed by the formation of a CH···O hydrogen bond. In this work we demonstrated that this interaction, previously observed in ethanol-d_6 as solvent [34], was preserved in D_2O solution and persisted upon aggregate formation. Since, especially for the aggregate form, the case of null NOE cross-peaks due to motional conditions could be verified, we also acquired ROESY spectra of LCOB 2.0×10^{-2} mol/dm^3 in D_2O at two different temperatures, confirming our previous findings (see Fig. F supplementary material).

Moreover, the interaction of the glucose H_1' with the bridge $H_{13\alpha,\beta}$ produced two peaks with different intensity (Fig. 3B). This suggested that the rotation of glycosidic C_1'–C_{13} was also restricted, probably because of the formation of an additional hydrogen bond between $O_2'H$ and O_1' giving an interaction which takes advantage of the co-operative properties of H-bond [47].

All these experimental data were compared with the model obtained by DFT calculation. Fig. 6 reports the optimised structure of LCOB from which the following information were extracted: i) the distance between C_2 and O_1' (2.81 Å) was lower than the sum of their Van der Waals radius (3.1 Å), confirming the presence of a CH···O bond (distance H_2–O_1' = 2.51 Å). ii) the distance between O_2' and O_1' (2.90 Å) was closer than the sum of their Van der Waals radius, (H_2'–O_1' = 2.60 Å), suggesting also in this case the presence of a hydrogen bond. iii) At the same time it was evident that, in this conformation, the distances H_1'–$H_{13\alpha}$ and H_1'–$H_{13\beta}$ were considerably dissimilar (2.53 Å and 3.06 Å, respectively), which was consistent with the different intensity of the respective NOESY cross-peaks described above. In summary, the theoretical model very well matched the hypothetic structure depicted by NMR experimental data.

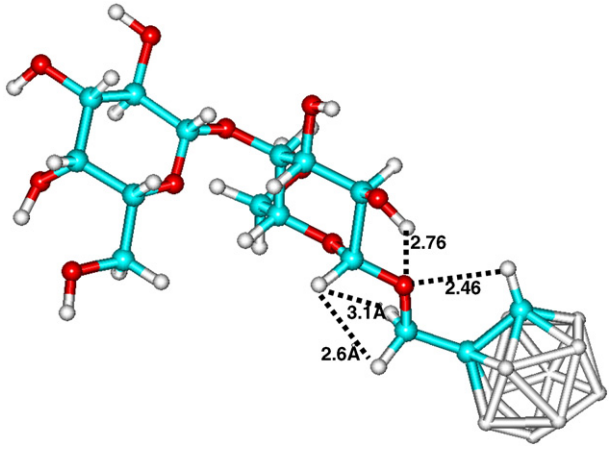

Fig. 6. *Ab-initio* optimised structure of LCOB model. The values for H_2–O_1', H_1'–O_1', H_1'–$H_{13\alpha}$ and H_1'–$H_{13\beta}$ inter-atomic distances are reported. Hydrogens of the cage were omitted for clarity.

4. Conclusions

In this paper the structural and dynamic properties of a dicarba-*closo*-dodecaborane functionalised with the lactose disaccharide, were analysed in water solution. This molecule, potentially active for BNCT, showed amphiphilic characteristics which were deeply investigated, both in the aggregate and non-aggregate form. Comparison was made with data acquired in ethanol solution.

LCOB showed meaningful differences from classical surfactants. These molecules possess a flexible hydrocarbon chain, and usually show structural changes which take place as a consequence of micelle formation [48,49]. Moreover, segmental motion and lateral diffusion strongly affect relaxation parameters. The characteristic of classical surfactants was not observed for LCOB aggregates in D_2O. On the other hand, kinetic aspects, characterized by a rapid exchange with the bulk monomers, dominated the whole dynamic behaviour of LCOB aggregates. High sensitivity of the aggregate kinetics with respect to temperature conditions was also observed.

Temperature variations and aggregate formation were not able to disrupt the observed intra-molecular CH···O bond and did not introduce any substantial change at the molecular level. This confirmed the unusual strength of this CH···O, as previously observed in different solvents [34,36]. Inter-molecular

CH···O interactions were not evidenced in the aggregates, probably because unfavoured by entropic factors. This also suggested that non-specific hydrophobic effects were the primary driving force for aggregate formation.

Acknowledgments

Thanks are due to the Ministero dell'Istruzione, dell'Università e della Ricerca Scientifica and to Italian Inter-University Consortium Sistemi a Grande Interfase (CSGI) for the financial support. Thanks are also due to the European Center for Magnetic Resonance (CERM) in Florence for the use of NMR spectrometer equipped with the cryoprobe.

Appendix A. Supplementary data

Supplementary data associated with this article can be found, in the online version, at doi:10.1016/j.bpc.2006.09.004.

References

[1] R.E. Williams, The polyborane, carborane, carbocation continuum: architectural patterns, Chem. Rev. 92 (1992) 177–207.
[2] R.B. King, Three-dimensional aromaticity in polyhedral boranes and related molecules, Chem. Rev. 101 (2001) 1119–1152.
[3] V.I. Bregadze, Dicarba-*closo*-dodecaboranes C2B10H12 and their derivatives, Chem. Rev. 92 (1992) 209–223.
[4] R.A. Watson-Clark, M.F. Hawthorne, An exploratory evaluation of the reactions of organic oxidants with polyhedral borane anions, Inorg. Chem. 36 (1997) 5419–5420.
[5] L.J. Yeager, F. Saeki, K. Shelly, M.F. Hawthorne, R.L. Garrell, A new class of self-assembled monolayers: *closo*-$B_{12}H_{11}S^{3-}$ on Gold, J. Am. Chem. Soc. 120 (1998) 9961–9962.
[6] Y. Mishima (Ed.), Cancer Neutron Capture Therapy, Plenum Press, New York, 1996.
[7] M.F. Hawthorne, A. Madema, Applications of radiolabeled boron clusters to the diagnosis and treatment of cancer, Chem. Rev. 99 (1999) 3421–3434.
[8] R.F. Barth, J.A. Coderre, M.G.H. Vicente, T.E. Blue, Boron neutron capture therapy of cancer: current status and future prospects, Clin. Cancer Res. 11 (2005) 3987–4002.
[9] Y. Mishima, C. Honda, M. Ichihashi, H. Obara, J. Hiratsuka, H. Fukuda, H. Karashima, T. Koboyashi, K. Kanda, K. Yoshino, Treatment of malignant melanoma by single thermal neutron capture therapy with melanoma-seeking 10B-compound, Lancet 2 (1989) 388–389.
[10] J.A. Coderre, J.D. Glass, R.G. Fairchild, P.L. Micca, I. Fand, D.D. Joel, Selective delivery of boron by the melanin precursor analogue *p*-boronophenylalanine to tumors other than melanoma, Cancer Res. 50 (1990) 138–141.
[11] L.F. Tietze, U. Bothe, Ortho-carboranyl glycosides of glucose, mannose, maltose and lactose for cancer treatment by boron neutron-capture therapy, Chem. Eur. J. 4 (1998) 1179–1183.
[12] G.B. Giovenzana, L. Lay, D. Monti, G. Palmisano, L. Panza, G.B. Giovenzana, L. Lay, D. Monti, G. Palmisano, L. Panza, Synthesis of carboranyl derivatives of alkynyl glycosides as potential BNCT agents, Tetrahedron 55 (1999) 14123–14136.
[13] L.F. Tietze, U. Bothe, I. Schuberth, L.F. Tietze, U. Bothe, I. Schuberth, Preparation of a new carboranyl lactoside for the treatment of cancer by boron neutron capture therapy: synthesis and toxicity of fluoro carboranyl glycosides for in vivo 19F NMR spectroscopy, Chem.-Eur. J. 6 (2000) 836–842.
[14] L.F. Tietze, U. Bothe, U. Griesbach, M. Nakaichi, T. Hasegawa, H. Nakamura, Y. Yamamoto, Ortho-carboranyl glycosides for the treatment of cancer by boron neutron capture therapy, Bioorg. Med. Chem. 9 (2001) 1747–1752.
[15] S. Morandi, S. Ristori, D. Berti, L. Panza, A. Becciolini, G. Martini, Association of sugar-based carboranes with cationic liposomes: an electron spin resonance and light scattering study, Biochim. Biophys. Acta 1664 (2004) 53–63.
[16] S. Rossi, G. Karlsson, G. Martini, K. Edwards, Combined cryogenic transmission electron microscopy and electron spin resonance studies of epc liposomes loaded with carboranyl compounds for BNCT, Langmuir 19 (2003) 5608–5617.
[17] S. Ristori, J. Oberdisse, I. Grillo, A. Donati, O. Spalla, Structural characterization of cationic liposomes loaded with sugar-based carboranes, Biophys. J. 88 (2005) 535–547.
[18] H. Wennerstrom, B. Lindman, O. Söderman, T. Drakenberg, B. Rosenholm, Carbon-13 magnetic relaxation in micellar solutions. Influence of aggregate motion on T_1, J. Am. Chem. Soc. 101 (1979) 6860–6864.
[19] B. Lindman, O. Söderman, H. Wennerström, in: R. Zana (Ed.), Surfactant Solutions: New Methods of Investigation, Surfactant Science Series, vol. 22, Marcel Dekker Inc., 1986.
[20] D.F. Evans, H. Wennerström, The Colloidal Domain: Where Physics, Chemistry, Biology, and Technology Meet, Wiley, Europe, 1999.
[21] S. Macura, K. Wüthrich, R.R. Ernst, Separation and suppression of coherent transfer effects in two-dimensional NOE and chemical exchange spectroscopy, J. Magn. Reson. 46 (1982) 269–282.
[22] A.A. Bothner-By, R.L. Stephens, R.L. Lee, C.D. Warren, R.W. Jeanloz, J. Am. Chem. Soc. 106 (1984) 811–813.
[23] U. Piantini, O.W. Sörensen, R.R. Ernst, Multiple quantum filters for elucidating NMR coupling networks, J. Am. Chem. Soc. 104 (1982) 6800–6801.
[24] D. Marion, K. Wutrich, Application of phase sensitive two-dimensional correlated spectroscopy (COSY) for measurement of ^1H–^1H spin–spin coupling constants in proteins, Biochem. Biophys. Res. Commum. 113 (1983) 967–974.
[25] A.J. Shaka, P.B. Barker, R. Freeman, Computer-optimized decoupling scheme for wideband applications and low-level operation, J. Magn. Reson. 64 (1985) 547–552.
[26] A.G. Palmer, J. Cavanagh, P.E. Wright, M. Rance, Sensitivity improvement in proton-detected two-dimensional heteronuclear correlation NMR spectroscopy, J. Magn. Reson. 93 (1991) 151–170.
[27] D.J. States, R.A. Haberkorn, D.J. Ruben, A two-dimensional nuclear Overhauser experiment with pure absorption phase in four quadrants, J. Magn. Reson. 48 (1982) 286–292.
[28] R.L. Vold, J.S. Waugh, M.P. Klein, D.E. Phelps, Measurement of spin relaxation in complex systems, J. Chem. Phys. 48 (1968) 3831–3832.
[29] A.J. Shaka, J. Keeler, R. Freeman, Evaluation of a new broadband decoupling sequence: WALTZ-16, J. Magn. Reson. 53 (1983) 313–340.
[30] F. Delaglio, S. Grzesiek, G. Vuister, G. Zhu, J. Pfeifer, A. Bax, NMRPipe: a multidimensional spectral processing system based on UNIX pipes, J. Biomol. NMR 6 (1995) 277–293.
[31] T.D. Goddard and D.G. Kneller, SPARKY program version (3.6), University of California, San Francisco.
[32] Gaussian 03, Revision B.05, M.J. Frisch, G.W. Trucks, H.B. Schlegel, G.E. Scuseria, M.A. Robb, J.R. Cheeseman, J.A. Montgomery, Jr., T. Vreven, K.N. Kudin, J.C. Burant, J.M. Millam, S.S. Iyengar, J.Tomasi, V.Barone, B. Mennucci, M. Cossi, G. Scalmani, N. Rega, G.A. Petersson, H. Nakatsuji, M. Hada, M. Ehara, K. Toyota, R. Fukuda, J. Hasegawa, M. Ishida, T. Nakajima, Y. Honda, O. Kitao, H. Nakai, M. Klene, X. Li, J.E. Knox, H.P. Hratchian, J.B. Cross, V. Bakken, C. Adamo, J. Jaramillo, R. Gomperts, R.E. Stratmann, O. Yazyev, A.J. Austin, R. Cammi, C. Pomelli, J.W. Ochterski, P.Y. Ayala, K. Morokuma, G.A. Voth, P. Salvador, J.J. Dannenberg, V.G. Zakrzewski, S. Dapprich, A.D. Daniels, M.C. Strain, O. Farkas, D.K. Malick, A.D. Rabuck, K. Raghavachari, J.B. Foresman, J.V. Ortiz, Q. Cui, A.G. Baboul, S. Clifford, J. Cioslowski, B.B. Stefanov, G. Liu, A. Liashenko, P. Piskorz, I. Komaromi, R.L. Martin, D.J. Fox, T. Keith, M.A. Al-Laham, C.Y. Peng, A. Nanayakkara, M. Challacombe, P.M.W. Gill, B. Johnson, W. Chen, M.W. Wong, C. Gonzalez, and J.A. Pople, Gaussian, Inc., Wallingford CT, 2004.
[33] IBM SP5/512 high performance computer at CINECA Computer Center, Casalecchio di Reno, Bologna, Italy.

[34] A. Donati, S. Ristori, C. Bonechi, L. Panza, G. Martini, C. Rossi, Evidences of strong C–H…O bond in an *o*-Carboranyl *β*-Lactoside in solution, J. Am. Chem. Soc. 124 (2002) 8778–8779.
[35] S. Heømánek, Boron-11 NMR spectra of boranes, main-group hetero-boranes, and substituted derivatives. Factors influencing chemical shifts of skeletal atoms, Chem. Rev. 92 (1992) 325–362.
[36] A. Cappelli, G. Giorgi, M. Anzini, S. Vomero, S. Ristori, C. Rossi, A. Donati, Characterization of persistent intramolecular C–H···X(N,O) bonds in solid state and solution, Chem.-Eur. J. 10 (2004) 3177–3183.
[37] G.R. Desiraju, The C–H···O hydrogen bond: structural implications and supramolecular design, Acc. Chem. Res. 29 (1996) 441–449.
[38] M.H. Levitt, Spin Dynamic — Basics of Nuclear Magnetic Resonance, J. Wiley & Sons ltd, Chichester, 2002.
[39] Calculated for 2.0Å inter-proton distance and 11.7 T as static magnetic field.
[40] D. Neuhaus, M.P. Williamson, The nuclear Overhauser effect in: Structural and Conformational Analysis, VCH Publishers, New York, 1989.
[41] F. Heatley, ^{13}C longitudinal and transverse magnetic relaxation in micellar and non-micellar sodium octanoate, J. Chem. Soc. Faraday Trans. 83 (1987) 2593–2603.
[42] O. Söderman, G. Carlström, M. Monduzzi, U. Olssön, NMR relaxation in micelles formed by a long zwitterionic surfactant, Langmuir 4 (1988) 1039–1044.
[43] A. Ceglie, M. Monduzzi, O. Söderman, A ^{2}H and ^{13}C NMR multifield relaxation study of some nonaqueous systems of sodium dodecyl sulfate, J. Colloid Interface Sci. 142 (1991) 129–139.
[44] I. Furò, R. Sitnikov, Order parameter profile of perfluorinated chains in a micelle, Langmuir 15 (1999) 2669–2673.
[45] M. Ueno, Y. Takamura, S. Nagadome, G. Sugihara, K. Takahashi, NMR study of bile salts' molecules in binary mixed micelles of bile salt and a non-ionic surfactant, Colloids Surf., B Biointerfaces 19 (2000) 43–54.
[46] G.M. Clore, A.M. Gronenborn, Theory and applications of the transferred NOE. Effects to the study of the conformations of small ligands bound to proteins, J. Magn. Reson. 48 (1982) 402–417.
[47] T. Steiner, W. Saenger, Role of C–H···O hydrogen bonds in the coordination of water molecules. Analysis of neutron diffraction data, J. Am. Chem. Soc. 115 (1993) 4540–4547.
[48] S. Borocci, G. Mancini, G. Cerichelli, L. Luchetti, Conformational behavior of aqueous micelles of sodium *N*-Dodecanoyl-L-prolinate, Langmuir 15 (1999) 2627–2630.
[49] H.Z. Yuan, G.Z. Cheng, S. Zhao, X.J. Miao, J.Y. Yu, L.F. Shen, Y.R. Du, Conformational dependence of Triton X-100 on environment studied by 2D NOESY and ^{1}H NMR relaxation, Langmuir 16 (2000) 3030–3035.